Eur. Phys. J. B **42**, 47–50 (2004)
DOI: 10.1140/epjb/e2004-00356-9

THE EUROPEAN PHYSICAL JOURNAL B

Microcavity strongly doped with CdSe nanocrystals

S. Rabaste[1], J. Bellessa[1,a], C. Bonnand[1], J.C. Plenet[1], and L. Spanhel[2]

[1] Laboratoire de Physique de la Matière Condensée et des Nanostructures, Université Claude Bernard Lyon 1, CNRS-UMR 5586, 43 boulevard du 11 Novembre, 69622 Villeurbanne Cedex, France
[2] Laboratoire Verres et Céramiques, CNRS-UMR 6512, Institut de Chimie de Rennes, Université de Rennes 1, CS 74205 35042 Rennes Cedex, France

Received 23 July 2004
Published online 26 November 2004 –

Abstract. The fabrication and the study of sol gel-microcavities strongly doped with CdSe nanocrystals are presented. The Fabry-Perot microcavities are formed by a Distributed Bragg Reflector covered with a CdSe doped active layer and a silver mirror. These microcavities are studied with reflectometry experiments. We observe that the cavity resonance peak is enlarged by a factor two when his spectral position corresponds to the first absorption line of the CdSe nanocrystals. Transfer matrix method calculation taking into account the CdSe absorption have been performed and are in good agreement with the experimental values.

PACS. 78.67. Bf Nanocrystals and nanoparticules – 81.07.-b Nanoscale materials and structures: fabrication and characterization

1 Introduction

Semiconductor nanocrystals (NC), which are crystals of size comparable to the Bohr radius of excitons, are of increasing interest because their optical properties can be tailored by modifying their size. They are very promising to fabricate new optical devices, like single photon sources [1] or light emitting diodes [2]. The NC optical properties can also be modified by changing their environment. They have been, for example, included in planar microcavities and a highly directional emission has been observed [3,4]. The inclusion of NCs in photonics dot, formed by dielectric spheres, leads to modifications of the spontaneous emission rate [5,6]. All these experiments are achieved in a weak coupling regime, i.e. the damping prevails on the light matter interaction.

The inclusion of semiconductor NCs in sol gel layer has been used for guided wave experiments and non linear optics [7]. One of the advantages of the sol-gel technique to obtain optical thin film is the large concentration of doping materials which can be achieved in the sol-gel films. This technique is also very efficient to fabricate planar microcavities [8]. The aim of this work is to increase the nanocrystals concentration in a microcavity and to study the cavity/nanocrystals interaction. In our case a spectrally thin cavity resonance interacts with a nanocristals first absorption line ten times larger. The spectral modifications of the cavity resonance, due to the NCs, have been studied and present a different behavior as the one obtained for weakly coupled NCs.

[a] e-mail: bellessa@lpmcn.univ-lyon1.fr

In Section 2 of this paper the fabrication of a microcavity by a sol-gel process and the synthesis of CdSe nanocrystals by a colloid chemical method, are exposed. The optical study, with reflectometry experiment, of these structures will be presented in Section 3. Finally a comparison between experimental results and calculations using transfer matrix method will be presented and a discussion about the inhomogeneous broadening of the absorption line will close this work.

2 Fabrication of the microcavity

The cavities studied are formed by an active layer, doped with CdSe nanocrystals, inserted between a sol-gel Bragg mirror and a metallic mirror. The first mirror is a Distributed Bragg Reflector (DBR). DBRs are constituted of alternated high and low index quarter wave layers of TiO_2 and SiO_2 which exhibit a refractive index of 2.30 and 1.46 at a wavelength of 500 nm, respectively. The TiO_2 sol was prepared by mixing titanium isopropoxyde and propanol-2. Acetic acid was added to prevent the precipitation of TiO_2. Finally, methanol is used as solvent [9]. For the SiO_2 sol preparation, tetra ethyl ortho silicate (TEOS) is mixed with chloric acid and diluted in ethanol [10]. Films are deposited by a dip coating technique under controlled air humidity, onto optically polished silicon wafers. After each layer deposition, the films were dried at 100 °C in order to evaporate the more volatile solvents and annealed at 350 °C during 5 minutes to burn out the organic residues. All the thermal

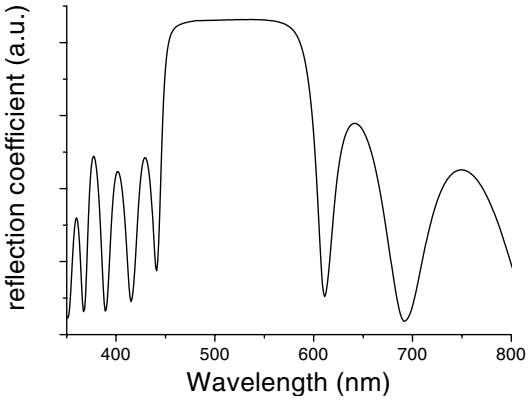

Fig. 1. Reflectivity spectrum of a sol-gel DBR constituted with 7 pairs of alternative TiO_2 and SiO_2 layers.

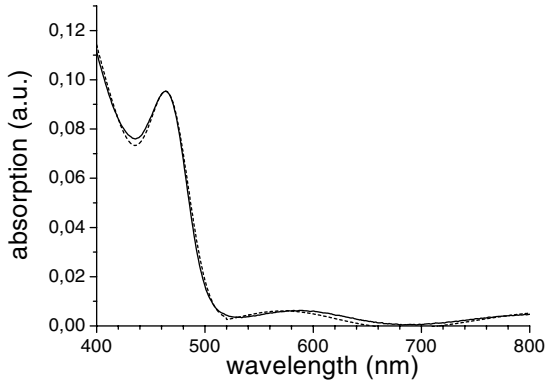

Fig. 2. Absorption spectrum of a CdSe doped ZrO_2 layer, in full line, deposited on a glass substrate and fabricated in the same condition as the NC doped layer inserted in the microcavity. The dashed line shows a calculated absorption of the layer, with a transfer matrix method.

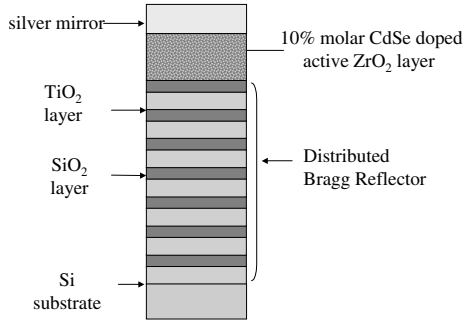

Fig. 3. Layout of the NCs doped microcavities.

treatments are realized with a Rapid Thermal Annealing furnace (JETFIRST 100, JIPELEC). To annihilate the mechanical stresses in the stacked layers, a very short firing at 900 °C is performed after the formation of each pair of TiO_2 and SiO_2 layers. Details of this process are given in the reference [11].

For the microcavity studied, the DBR is constituted by the stack of 7 pairs of alternative layers of SiO_2 and TiO_2. The reflectance spectrum of a single DBR has been measured with a reflection angle of 3°, and is shown in Figure 1. The stop-band ranges from 450 nm to 610 nm. The maximum of reflectivity is centered at 510 nm and the reflectivity value deduced from cavity measurements [8] is 99.7%.

The second step to fabricate the microcavity is the formation of the nanocristals doped layer. CdSe nanocrystals have been synthesized with a colloidal chemical process. Our method can be described in three steps: first, selenide powder is dissolved in a solution composed by Aminopropyltriethoxysilan (AMEO) and Mercaptopropyl triethoxysilan (MPTS) under dry atmosphere, to prevent the oxidation of the Se powder. The second step consists in the dissolution of anhydrous Cadmium Chloride ($CdCl_2$) powder in AMEO and butoxyethanol. This solution is heated up during 3 hours at 170 °C under reflux. Finally, both solutions are mixed under Argon atmosphere at room temperature. The resulting CdSe nanocrystals solution is yellow.

The CdSe nanocrystals have been included in a ZrO_2 sol-gel matrix. The ZrO_2 sol has been obtained by mixing Zirconium propoxyde, Acetylaceton and isopropanol [12]. We have used a doping rate in concentration of $\frac{n_{CdSe}}{n_{ZrO_2}} = 0.1$. For greater molar ratio, an enlargement of the CdSe absorption line appears, due to the interaction between the CdSe nanocrystals. The active layer of the microcavity was dip coated on the DBR and heat treated at 100 °C to evaporate the solvents. Its thickness is such as the resonance wavelength of the cavity in normal incidence is just above the CdSe absorption edge. Figure 2 shows an absorption spectrum of a CdSe doped ZrO_2 layer deposited on a glass substrate. This layer has been fabricated in the same conditions as the layers used in the microcavities. Two parts can be separated in this spectrum: for wavelengths lower than 520 nm the absorption of the nanocrystals is the main contribution. The maximum of the first absorption line lies at 466 nm, its Full at Maximum Half Width (FMHW) is 34 nm, and for smaller wavelengths the absorption increases. The comparison with absorption energy calculations of the CdSe nanocrystals shows that the average diameter of the quantum dots is about 2 nm [13]. For wavelengths larger than 520 nm, the absorption of the nanocrystals is very low. This is confirmed by absorption measurements performed on liquid nanocrystals solutions. The oscillations in the transmission spectrum of the doped layer are related to interferometric phenomena, and the positions of the maxima and minima are directly correlated to the optical thickness of the layer. A transfer matrix method simulation leads to a thickness of the layer of 600 nm. A simulated transmission of a ZrO_2 layer doped with nanocrystals is shown in Figure 2 in dashed lines. The complex optical index used in this simulation (real for wavelengths greater than 520 nm) is described in the Section 4 of the article.

To close the microcavity, a silver thin film is deposited by electron gun evaporation under a vacuum of 10^{-6} torr. The deposed thickness is 38 nm. Figure 3 shows a layout of the microcavity described above.

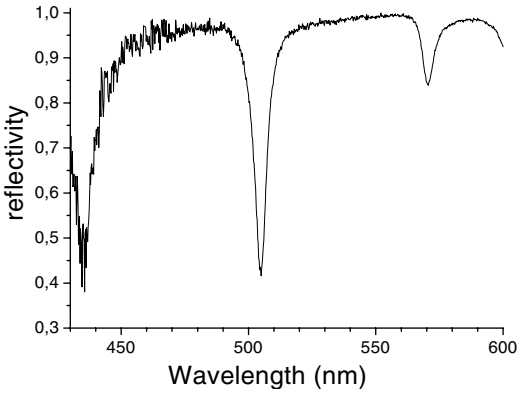

Fig. 4. Reflectivity spectrum versus the wavelength of a CdSe NCs doped microcavity with a reflection angle $\theta = 10°$.

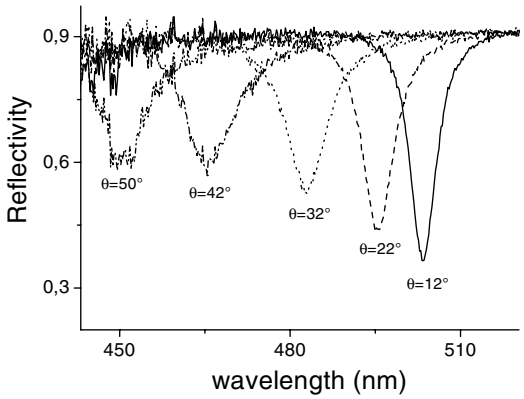

Fig. 5. Central part of the reflectivity spectra of a microcavity for 5 angles of reflection (θ).

3 Optical studies

To measure the interaction between the nanocrystals and the cavity, reflectometry experiments have been performed. The resonance wavelength of the cavity has been tuned, by changing the reflectivity angle, to cross the nanocrystals absorption. For low reflection angles the cavity resonance wavelength is greater than the NCs absorption wavelength and reaches the first absorption line when the angle increases. The sample has been mounted on a $\theta - 2\theta$ rotating table. The light source is a quartz lamp coupled to a Jobin Yvon Triax 320 monochromator. The light is focused on the top of the sample (silver layer) and detected, after reflection, with a Si diode and a lock-in amplifier. The reflectivity versus the wavelength of a strongly doped microcavity, for an incidence angle of 10°, is shown in Figure 4. Three dips are visible on the spectrum, the peaks situated at 440 nm and 570 nm are related to the reflectivity minima of the DBR. The 505 nm dip is related to the cavity resonance and is in the middle of the stopband of the DBR. The FWHM of the resonant peak is 5 nm corresponding to a cavity quality factor of 100.

Figure 5 shows the central part of reflectivity spectra recorded for different detection angles. A modification of the dip width appears clearly on these spectra. For $\theta = 10°$, the resonance is located at 505 nm where the CdSe absorption is low. The dip width increases until $\theta = 42°$ corresponding to a resonance at 465 nm, which is the maximun of the first CdSe absorption line. The Dip FWHM decreases for $\theta = 50°$ in the same manner as the CdSe absorption. A decrease of the dip depth occurs when the angle increases and can also be related to the CdSe absorption.

4 Discussion

To understand the shape modification of the cavity resonance dips, the reflectometry results have been compared to simulation obtained with a transfer matrix method [14]. To take into account the CdSe absorption, a complex optical index has been used. The CdSe nanocrystals absorption spectrum is calculated as a sum of a Gaussian function for the first absorption line and a polynomial function for the contribution of the other transitions of greater energies, then, the imaginary part of the optical index is given by $A = \frac{4\pi}{\lambda}k$, with A the absorption coefficient, λ the wavelength and k the imaginary part of the index. The real part of the index is obtained with a Kramers Kronig transformation. In order to check the complex index obtained, the calculated transmission of a single CdSe doped layer deposited on a glass substrate is compared to the experimental transmission, as shown in Figure 1. The simulation is in good agreement with the experimental values. The same complex index has been used to calculate the microcavity reflection coefficient.

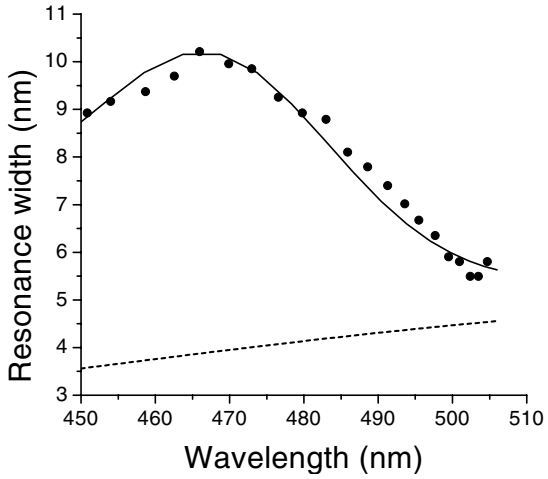

Fig. 6. Experimental value of the FWHM of the resonant peak versus the resonance wavelength in black circles; the calculated values of the resonance FWHM of a doped microcavity is shown in full line and in dashed line for an undoped microcavity.

For different detection angles, experimental and calculated reflectivities of the CdSe doped microcavities have been compared. Figure 6 shows the evolution of the FWHM of the resonance peaks versus the wavelength, for the calculated and measured cases. The calculated FWHM of the resonant peaks of an empty cavity is presented as reference. This last curve shows that if there is no coupling between the microcavity and the nanocrystals,

a little linear variation of the FWHM occurs (less than one nanometer) when the resonant angle increases, probably due to index modifications of the silver and dielectric layers when the resonance wavelength is modified. If we take into account the nanocrystals, the calculated FWHM is largely enlarged: from 5 nm to more than 10 nm. A good agreement between the calculated and experimental values is obtained as shown in Figure 6 and the resonance shape modification is clearly related to the absorption of the nanocrystals.

In a cavity weak coupling regime, the shape of the cavity resonance is not modified due to the material in the cavity. The cavity changes the spontaneous emission rate of the NCs but the energy position of the peak should be unchanged. Another interaction regime between an emitter and a cavity is the strong coupling regime. In this case, an anticrossing in the dispersion relations occurs and this is not our case. The interaction is in an intermediate regime, resulting of the interaction of a sharp line, the cavity resonance, with a very large line, the NCs absorption. The NC-cavity interaction lead to a modification smaller than the NC width but larger than the microcavity resonance (the width is multiplied by more than a factor 2) and the difference between the coupled and uncoupled FWHM is 6.5 nm at a wavelength of 467 nm.

The large width of the nanocrystals absorption is due to an inhomogeneous broadening induced by the size distribution of the nanocrystals. The NC homogeneous width has been measured at room temperature at 50 meV [15] which corresponds to 9 nm in our case, compared to a total width of 32 nm for the first absorption line.

The comparison of the calculated and measured data shows that the cavity resonance width enlargement can be well fitted with a transfer matrix method. The calculation using a complex index to describe the absorbing material in the cavity has been shown to give very good result for homogeneous broadening [16] and this calculation does not take into account the nature of the absorption line, homogeneous or inhomogeneous. The enlargement obtained would be the same with an homogeneous line at 465 nm with a 32 nm FWHM. We can conclude that the inhomogeneous nature of the broadening does not modify the enlargement of the cavity resonance observed, although the cavity width enlargement (6.5 nm) is of the same order of magnitude as the homogeneous width and the cavity uncoupled resonance width.

5 Conclusion

In conclusion the fabrication of sol-gel microcavities doped with CdSe nanocrystals has been described. The optical properties of such cavities have been studied showing an enlargement of the cavity resonance width when this resonance is accorded to the NC first absorption line. Calculations using a transfer matrix method with a complex index for the NC doped layer have been performed and are in good agreement with the experimental results. The calculations are independent of the nature of the line, homogeneous or inhomogeneous, and are very adapted to homogeneous lines. This shows that the inhomogeneous line broadening of the CdSe absorption line does not induce modification of the optical properties of the cavity and that the same result would have been obtained with an homogeneous line.

References

1. P. Michler, A. Imamoglu, M.D. Mason, P.J. Carson, G.F. Strouse, S.K. Buratto, Nature **406**, 968 (2000)
2. V.L. Colvin, M.C. Schlamp, A.P. Alivisatos, Nature (London) **370**, 354 (1994)
3. C.E. Finlayson, D.S. Ginger, N.C. Greenham, Appl. Phys. Lett. **77**, 2500 (2000)
4. J. Roither, W. Heis, D.V. Talapin, N. Gaponik, A. Eychmuller, Appl. Phys. Lett. **84**, 2223 (2004)
5. M.V. Artemyev, U. Woggon, Appl. Phys. Lett. **76**, 2223 (2000)
6. X. Fan, M.C. Lonergan, Y. Zhang, H. Wang, Phys. Rev. B **64**, 115310 (2001)
7. S. Juodkazis, E. Bernstein, J.C. Plenet, C. Bovier, J.G. Dumas, J. Mugnier, J.V. Vaitkus, Opt. Commun. **148**, 142 (1998)
8. J. Bellessa, S. Rabaste, J.C. Plenet, J. Dumas, J. Mugnier, O. Marty, Appl. Phys. Lett. **79**, 2142 (2001)
9. A. Bahtat, M. Bouazaoui, M. Bahtat, C. Garapon, B. Jacquier, J. Mugnier, J. Non-Cryst. Solids **202**, 16 (1996)
10. K.A. Cerqua, W.C. LaCourse, J. Non-Cryst. Solids **100**, 471 (1988)
11. S. Rabaste, J. Bellessa, A. Brioude, C. Bovier, J.C. Plenet, R. Brenier, O. Marty, J. Mugnier, J. Dumas, Thin Solid Films **416**, 242 (2002)
12. C. Urlacher, J. Dumas, J. Serughetti, M. Munoz, J. Sol-Gel Sci. Technol. **8**, 999 (1997)
13. S.V. Gapnenko, *Optical Properties of Semiconductors Nanocrystals* (Cambridge University Press, Cambridge, 1998), pp. 90−91
14. M. Born, E. Wolf, *Principles of Optics*, 6th edn. (Pergamon Press, Oxford, 1980)
15. G. Schlegel, J. Bohnenberger, I. Potapova, A. Mews, Phys. Rev. Lett. **88**, 137401 (2002)
16. Y. Zhu, D.J. Gauthier, S.E. Morin, Q. Wu, H. Carmichael, T.W. Mossberg, Phys. Rev. Lett. **64**, 2499 (1990)